

# EXPERIMENTAL INVESTIGATION INTO ACOUSTIC CHARACTERISTICS OF LEAKAGE SIGNALS FROM UNDERWATER PLASTIC WATER-FILLED PIPES

Bin Liu<sup>1</sup>, Yan Gao<sup>1,2\*</sup>, Yifan Ma<sup>1,2</sup> and Jun Yang<sup>1,2</sup>

<sup>1</sup>*Key Laboratory of Noise and Vibration Research, Institute of Acoustics, Chinese Academy of Sciences, Beijing 100190 China*

<sup>2</sup>*University of Chinese Academy of Sciences, Beijing 100049 China*  
email: gaoyan@mail.ioa.ac.cn

Acoustic techniques based on cross-correlation are in common use for leak detection in water distribution pipes. However, little work has been done in underwater pipeline leak detection. This paper is concerned with experimental investigation into water leakage from a underwater plastic pipe, with particular emphasis on the acoustic characteristics of the propagating leak noise measured under controlled conditions, including the leak hole size, water pressure and submerged depth of the pipe. It is found that the leak noise from a submerged PE water pipe concentrates at low frequencies, with a flat spectrum that has been observed in the frequency range below 650 Hz. Experimental results demonstrate that the attenuation of a leak signal in the submerged water pipe is larger than the in-air case, whereas the propagation wavespeed is mainly affected by the pressure within the pipe. Specifically it is shown that for a lower pressure, the wavespeed is almost identical to that for the in-air water pipe; for a higher pressure, an increase in the wavespeed may occur. In this paper preliminary measurements are made, and test results show the detectability of the leakage from a submerged water pipe. Further work will be carried out to investigate the feasibility of the transient leak signals for online leak detection.

Keywords: underwater leakage, acoustic characteristics, attenuation, wavespeed

---

## 1. Introduction

Water pipelines are buried infrastructures to sustain modern life and economic growth. In recent years, accidents due to pipeline leakage, as a result of pipe aging and degradation, climate change and poor street work, have frequently attracted attention, resulting in wastage of energy and resources. Leakage detection and location from buried pipes are of great interest in China and across the globe. Currently available techniques for pipeline leak detection consist of non-acoustic and acoustic methods, with the latter having been shown to be effective and in common use within water leak detection community. Non-acoustic methods, for example ground penetrating radar [1], infrared thermography [2, 3], and mass/flow balance method have been adopted in some occasions and achieved varying degrees of success. In these methods, leakage can be detected by monitoring changes in the states of surrounding medium along the pipeline, or the parameters such as the flow, pressure and density of the contained water. Although they show some promise, it has practical issues of equipment deployment, reliability, ease of use and, of course cost.

Acoustic leak detection methods are based on the knowledge of propagation characteristics of leak noise. Popular methods are based on cross-correlation [4-6]. Another method, namely the negative pressure wave method, can be adopted to measure the transient leak signals for online leak detection, in particular in oil pipelines. In essence, a leak from a water supply pipe system generates noise, which can propagate along the pipeline with acoustic characteristics largely affected by the presence of the surrounding medium and contained fluid. Specifically for the water-filled pipe surrounded by a soil or water media, the characteristics of the leak signal in both the time and frequency domains are, to some extent, influenced by the factors such as the size of leak source, geometrical and material properties of the pipe and surrounding medium [7, 8]. There has been considerable research on accurate location of water leakage in buried pipes, based on some priori knowledge, principally the propagation speed of a leak. Attention also has been focused on leakage detection of underwater oil and gas pipes [9, 10]. Hunaidi and Chu [11] studied the acoustic characteristics of leak signals in buried plastic water pipes. However little work has been done on the leak signals from underwater water-filled pipes.

This paper is concerned with water leakage detection from an underwater PE pipe. In order to study the acoustic characteristics including the propagation wavespeed and attenuation of a leak signal, an experimental rig has been built. A number of preliminary measurements have been made and some results are reported in this paper. In the experiments, the leak noise signals were measured under controlled conditions of the leak hole size, water pressure and submerge depth of the pipe. The characteristics of leak signal are compared for different conditions in order to demonstrate what happens to the leak signals under these circumstances and hence the detectability of leak in practice.

## 2. Experimental setup

Tests were carried out at a leak detection pipe rig constructed at the campus of the Institute of Acoustics, Chinese Academy of Sciences. The general layout of the pipe and the data acquisition system are shown in Fig. 1. With reference to Fig. 1(a), the test rig comprised an approximately 40 m length of polyethylene (PE) pipe with diameter 110 mm and wall thickness 5 mm. Two valves were separately installed at the inlet and outlet. The BC section of about 5 m length of the pipe as plotted in Fig. 1(a), is placed in a water tank. Simulated leaks were generated by mounting copper covers with round holes of different sizes. Four B&K 8103 hydrophones (#1~#4) were installed at two sides of the leak source. The leak signals were collected by using a B&K PUSLE3050 system. The 20 s signals were each captured at the sampling frequency of 8192 Hz. They were high-pass filtered to reduce the interference due to ambient noise.

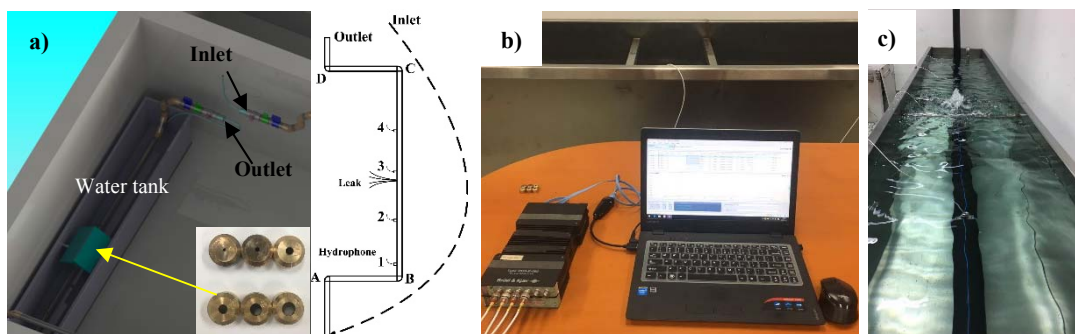


Figure 1: Experimental setup: a) Schematic of water pipeline; b) Data acquisition system; c) Underwater leakage.

## 3. Results and discussions

### 3.1 Time domain signal

Fig. 2 shows the background noise and leak signals measured by Hydrophone #3 (close to the leak source). The water pressure in the pipe was 0.04 MPa and the BC pipe section was submerged

at a depth of 15 cm (counting above the pipe). Three sizes of leak holes were tested with diameters 1 mm, 3 mm and 5 mm respectively. It can be seen from Fig. 2 that the magnitude of leak signal is much higher than the background noise, as anticipated. It increases with the leak size. However, limited information can be seen in the time domain. To better understand the characteristics of the leak signals, frequency analysis is required, and this is carried out as follows.

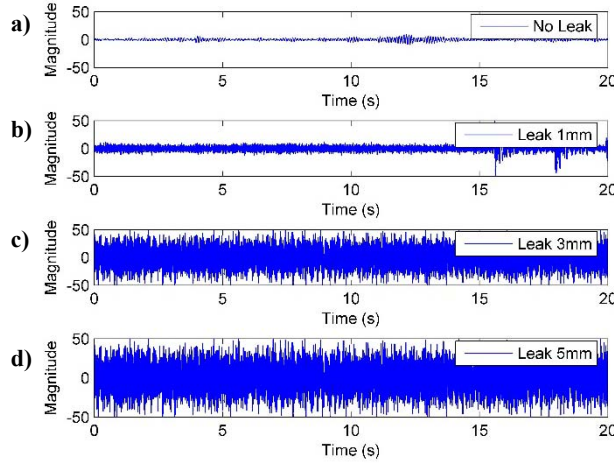


Figure 2: Time history signals measure by Hydrophone #3: (a) no leak; (b) leak hole of 1 mm; (c) leak hole of 3 mm; and (d) leak hole of 5 mm.

### 3.2 Auto-spectral densities of leak signals

Fig. 3 plots the auto-spectral densities (ASDs) of the background noise and leak signals from Hydrophones #1~#3. Again, the water pressure in the pipe was 0.04 MPa and the BC pipe section was submerged at a depth of 15 cm. Three sizes of leak holes were tested with diameters 1 mm, 3 mm and 5 mm respectively. It is clear from the figure that most of the energy is dominated by the background noise below 20 Hz. As discussed in the preceding subsection, the leak energy level largely increases compared to that without a leak, and slightly increases with the leak size. Comparing with the ASDs of leak signals at different locations and with different leak sizes, it can be found that the energy of the leak signals distribute in the low frequency range. Especially for the signal of Hydrophones #1 (Fig. 3(b)) and #2 (Fig. 3(c)), the ASDs drop to the background noise at about 500 Hz. This confirms that the leak signals are concentrated below this frequency, which is defined as a cut-off frequency ( $f_c$ ) of the leak signal in this paper. This finding is in consistent with previous research on buried plastic pipes [7, 8], i.e., the energy of leak signals from the underwater fluid-filled pipe lies in the low frequency range.

Above 500 Hz, comparison of the ASDs of leak signals measured by Hydrophones #1 and #2 shows that the distribution trend and the peak positions are almost the same. This indicates that pipe vibration dominates rather than the propagating leak signals. It is observed that for even higher frequencies above 2500 Hz, signals gradually drop to the level of the background noise.

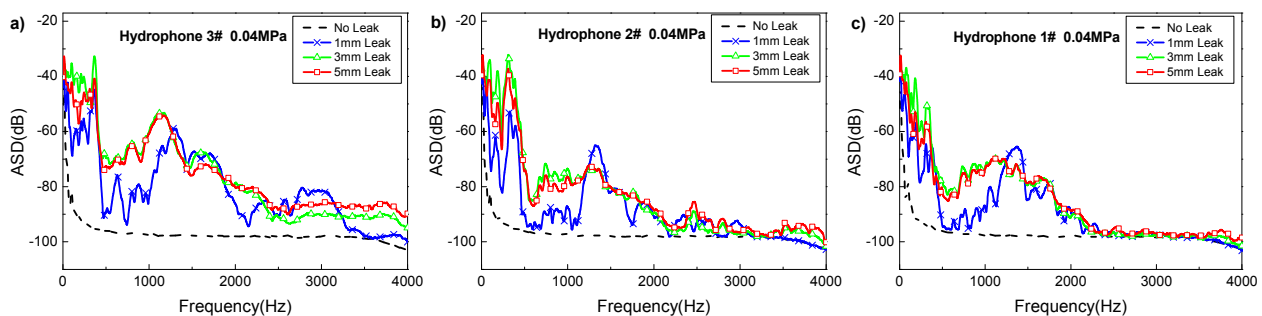


Figure 3: ASDs of hydrophone-measured signals: (a) close to the leak source (Hydrophone #3); (b) left side of leak source with a distance of 0.9 m (Hydrophone #2); and (c) left side of leak source with a distance of 1.9 m (Hydrophone #1).

Fig. 4 plots the ASDs measured by Hydrophone #3 under different water pressures. The pipe (BC section) was submerged at the depth of 15 cm and the diameter of leak hole was 3 mm. As can be seen from the figure, the ASDs of the leak signals and cut-off frequencies are highly influenced by the pressure within the pipe. The leak energy level rises dramatically with the increase of the water pressure from 0 to 0.04 MPa. This remain unchanged under higher water pressures.

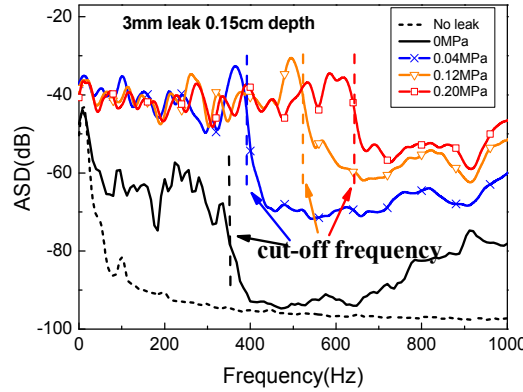


Figure 4: ASDs measured by Hydrophone #3 under different water pressures.

Interestingly, Fig. 4 shows that the leak signals have flat ASDs below the cut-off frequencies. This coincides with the assumption of the model for the leak noise propagation along plastic pipes in previous study by Gao et al [4-6]. The rationale behind this is beyond the scope of interest, and will be investigated in further work. In addition, the cut-off frequency increases slightly with the pressure within the pipe from 350 Hz to 650 Hz when the water pressure changes from 0 MPa to 0.20 MPa. This implies that the bandwidth of the leak signal become larger under higher water pressures.

Fig. 5 plots the ASDs of leak signals measure by Hydrophone #3 at different submerged depths of the pipe. The diameter of leak hole was 3 mm, and the water pressure was 0.20 MPa. Here the ASD results of leak signals are also plotted in comparison with the in-air case. It is shown in the figure that the ASD levels vary slightly for the submerged water pipe at different depths, whereas they are about 20 dB higher in the whole frequency range than the in-air case. Moreover, it is demonstrated that the leak energy concentrates in the low frequency range. The cut-off frequency is irrelevant to the submerged water depth, but it is slightly lower for the in-air water pipe.

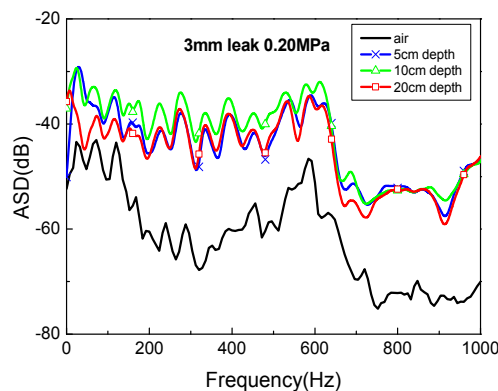


Figure 5: ASDs of leak signals measure by Hydrophone #3 at different submerged depths.

### 3.3 Attenuation

Attenuation rate is a reflective of the propagating distance of the leak signal at different frequencies in the pipe, and can be calculate by

$$Attenuation = \frac{-20\ln\{H\}}{D\ln 10} \quad (1)$$

where H is the transfer function between the sensor signal and the leak source signal; and D is the distance difference of the sensors from the leak source.

Fig. 6 shows the attenuation rates of leak signals at different submerged depths. It can be observed that the attenuation rate fluctuates and generally increases with frequency for the submerged water pipe, which is less dependent upon the submerged depths. In comparison, the attenuation for the in-air water pipe has almost the same level as the submerged case at low frequencies below 300Hz. Above this frequency, the attenuation level is much lower for the in-air water pipe, indicating the leak signals of this frequency range can be detected in a longer distance.

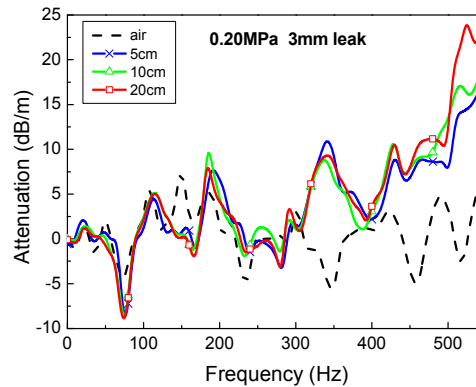


Figure 6: Attenuation rates of leak signals at different submerged depths.

### 3.4 Cross-spectral densities of leak signals

Fig. 7 shows the amplitude and phase of the cross-spectral densities (CSDs) between two signals measured by Hydrophones #1 and #3 for different leak hole sizes. The water pressure in the pipe was 0.04 MPa, and the submerged depth was 15 cm; the diameters of leak holes were 1 mm, 3 mm and 5 mm. It is clear from Fig. 7(a) that the leak signals have much higher CSD levels than the background noise. Referring to Fig. 7(b), the phase is approximately linear with frequency below 500 Hz, indicating the wavespeed of the leak signal can be calculated by the phase slope measured at the two positions [11]. It can be observed that the phase slope of different leak size is almost identical. This confirms the wavespeed is independent with the leak hole size. Further check of the corresponding coherence of the two leak signals as plotted in Fig. 8 shows that good coherence is achieved below 500 Hz when a leak occurs.

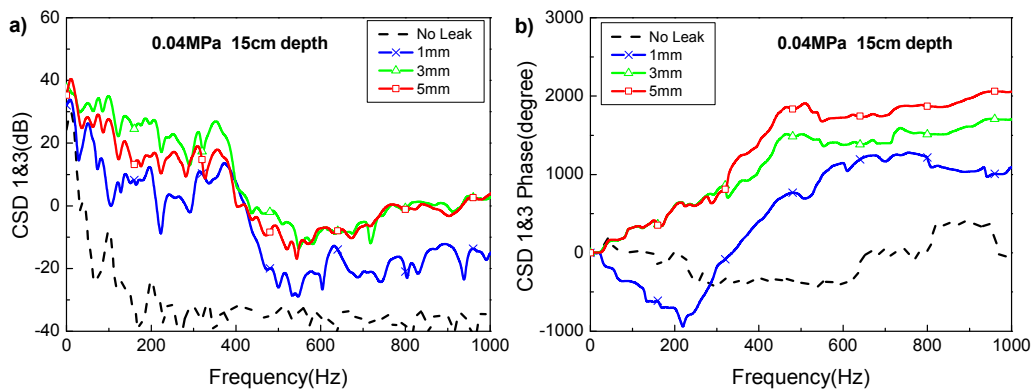


Figure 7: CSDs of the signals measured by Hydrophones #1 and #3 for different leak hole sizes: (a) Amplitude; and (b) Phase.

Fig. 9 plots the amplitude and phase of the CSDs between two signals measured by Hydrophones #1 and #3 under different water pressures. The diameter of leak hole was 3 mm, and the pipe (BC section) was submerged at a depth of 15 cm. The water pressures in the pipe varied from 0 MPa, 0.04 MPa, 0.12 MPa to 0.20 MPa. As shown in the figure, the energy of the leak signals is distributed in the low frequency range and the phase can clearly be seen to vary linearly with frequency, with a broader frequency range for higher water pressures with the upper frequencies marked as 300 Hz, 450 Hz and 650 Hz as shown in Fig. 9(b).



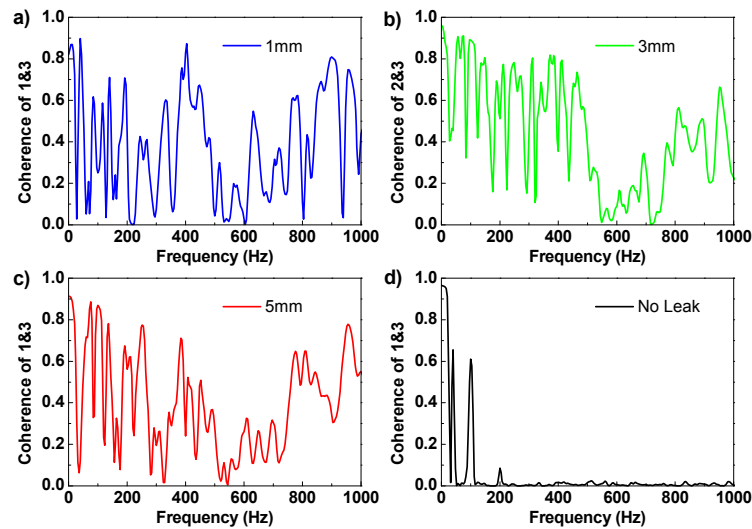


Figure 8: Coherence of leak signals measured by Hydrophones #1 and #3: (a) leak hole of 1mm; (b) leak hole of 3mm; (c) leak hole of 5mm; and (d) no leak.

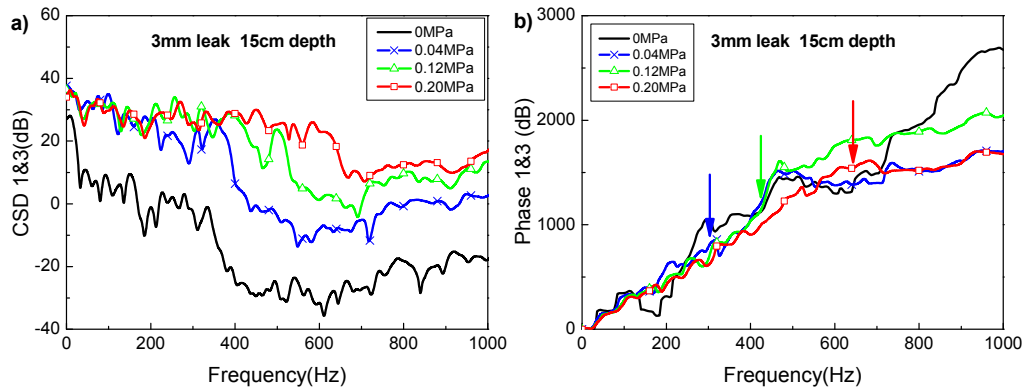


Figure 9: CSDs of the signals measured by Hydrophones #1 and #3 under different water pressures: (a) Amplitude; and (b) Phase.

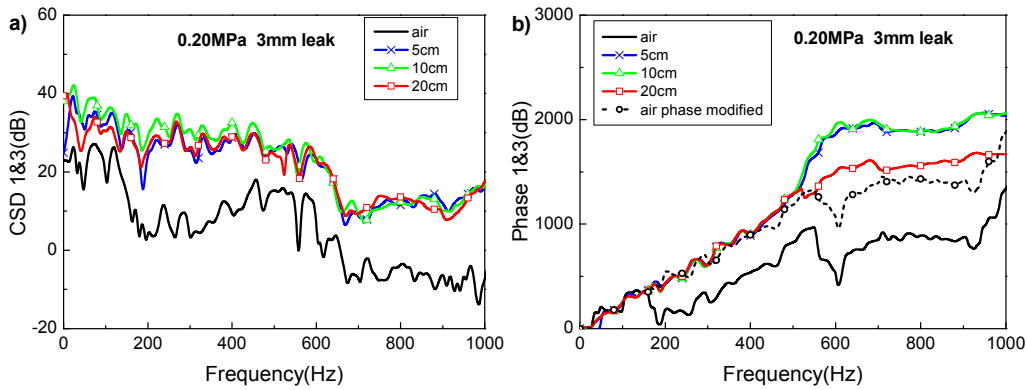


Figure 10: CSDs of the signals measured by Hydrophones #1 and #3 at different submerged depths: (a) Amplitude; and (b) Phase.

Fig. 10 shows the CSD of the signals measured by Hydrophones #1 and #3 at different submerged depths. The diameter of leak hole was 3 mm and the water pressure in the pipe was 0.20 MPa. The pipe (BC section) was submerged at the depths of 5 cm, 10 cm, 20 cm. The results of the in-air water pipe are also plotted in comparison. It is obvious that the submerged water pipe leads to a higher CSD level compared to the in-air case. A linear phase relationship is found below 500 Hz for both the submerged and in-air (except the sudden phase change of  $360^\circ$  at 150 Hz due to resonance [12]). After the phase modification, it can be observed that the phase slopes are identical with each other, which means the wavespeed is independent with the submerged depth.

### 3.5 Wavespeed

For leak detection based on cross-correlation to be effective, the propagation wavespeed of the leak must be known as a priori. Pinnington proposed a formula for calculating the wavespeed of the in-air fluid-filled pipe [13]

$$c = c_f \left( 1 + \frac{2Ba}{Eh} \right)^{-1/2} \quad (2)$$

where  $C_f$  is the free-filled wavespeed in water,  $B$  is the bulk modulus of the contained fluid, and hence  $B=2.25$  GPa and  $C_f=1500$  m/s for the water medium;  $a$  and  $h$  are the mean pipe radius and the wall thickness respectively;  $E$  is the elastic modulus of the pipe material. Here  $a=50$  mm,  $h= 5$ mm  $E=1.1$  GPa. From Eq. (2), the wavespeed is calculated as 231.7 m/s. Recent study by Gao et al [8] has shown that the leak signals travels slightly slower in the submerged pipe than in the in-air water pipe. However at the very low frequencies, the effect of surrounded medium on the wavespeed can be neglected.

The measured wavespeed in the pipe can be obtained from the phase of the CSD of two leak signals by [11]

$$V = 360d/k \quad (3)$$

where  $d$  is the distance difference between two sensor positions; and  $k$  is the slope of the phase ( $^{\circ}$ /Hz).

The above analysis suggests that the optimal frequency range and the phase slope are independent with the leak hole size and the submerged depth. The frequency range is appropriately selected based on the amplitude and phase of the CSD under different water pressures. Table 1 lists the calculated wavespeed given the recommended frequency ranges. It can be observed that the wavespeed is in 230m/s~260m/s, which is approximately in accordance with the theoretical result under lower water pressures and slightly higher under higher water pressures.

Table 1: Wavespeed calculated under different water pressures

Water pressure (MPa)	Recommended frequency range (Hz)	Wavespeed (m/s)
0	30-120	234
0.04	30-300	234
0.08	30-350	243
0.12	30-450	264
0.16	30-500	264
0.2	30-650	261

## 4. Conclusion

This paper presents the preliminary results of the acoustic characteristics of the leakage from a submerged PE water pipe. Experimental work has been carried out on the leak noise signals measured under controlled conditions, including the leak size, water pressure and submerged depth of the pipe, from which the wavespeed and the attenuation of the propagating leak signals along the pipe are obtained based on the frequency analysis. The main findings are

(1) The background noise has a much smaller energy level than the leak signal, which dominates the low frequencies below 20 Hz;

(2) A leak signal has a cut-off frequency, which lies in 350 Hz-650 Hz for this specific pipe rig. Below this frequency, the leak signal behaves as white noise with a flat spectrum. The energy level reduces greatly by 20~30 dB above this frequency;

(3) In general the larger the pressure within the pipe, the higher the cut-off frequency, and hence the wider frequency band of the leak signal;

(4) The attenuation of a leak signal in the submerged water pipe is larger than the in-air case;

(5) The wavespeed is independent with the leak hole size and the submerged depth. It is only affected by the pressure within the pipe. For a lower pressure, it can be estimated by the theoretical formula of the in-air case. A slight increase in the wavespeed is found for a higher water pressure.

The experimental work has clearly demonstrated that the leakage from the submerged water pipes is detectable. However the leak detection range can be significantly reduced due to higher attenuation. A model of acoustic characteristics of leakage in a submerged fluid-filled pipe is under way, which will be reported at a future date. Further work will also be carried out to investigate the feasibility of the transient leak signals for online leak detection.

## Acknowledgement

The authors thank the financial support of the CAS Hundred Talents Programme. Many thanks are also due to Prof. Chen Xiaobin and Mr. Gong Yangjun for their help in the design and construction of the experiment rig.

## REFERENCES

- 1 Lai W., Chang R., Sham J., et al, Perturbation mapping of water leak in buried water pipes via laboratory validation experiments with high-frequency ground penetrating radar (GPR), *Tunnelling and Underground Space Technology*, 52, 157-167, (2016).
- 2 Shen G. T., Li T., Infrared thermography for high-temperature pressure pipe, *INSIGHT*, 49(3), 151-153, (2007).
- 3 Manekiya M. H., Arulmozhivarman P., Leakage Detection and Estimation using IR Thermography, *2016 International Conference on Communication and Signal Processing (ICCSP)*, 1, 1516-1519, (2016).
- 4 Gao, Y., Brennan, M. J., Joseph, P. F., A comparison of time delay estimators for the detection of leak noise signals in plastic water distribution pipes, *Journal of Sound and Vibration*, 292, 552-570, (2006).
- 5 Gao, Y., Brennan, M. J., Joseph, P. F., et al, On the selection of acoustic/vibration sensors for leak detection in plastic water pipes, *Journal of Sound and Vibration*, 283, 927-941, (2005).
- 6 Gao, Y., Brennan, M. J., Joseph, P. F., et al, A model of the correlation function of leak noise in buried plastic pipes, *Journal of Sound and Vibration*, 277, 133-148, (2004).
- 7 Gao Y., Sui F., Muggleton J. M., et al, Simplified dispersion relationships for fluid-dominated axisymmetric wave motion in buried fluid-filled pipes, *Journal of Sound and Vibration*, 375, 386-402, (2016).
- 8 Gao Y., Liu Y., Muggleton J.M., Axisymmetric fluid-dominated wave in fluid-filled plastic pipes: loading effects of surrounding elastic medium, *Applied Acoustics*, 116, 43-49, (2017).
- 9 Wang Q., Wang X., Underwater Natural Gas Pipeline Leakage Detection based on Interferometric Fiber Optic Sensor in Experiment-scale, *22nd Chinese Control and Decision Conference*, 257-260, (2010).
- 10 Maksimov A. O., Polovinka Y. A., Time reversal technique for gas leakage detection, *Journal of the Acoustical Society of America*, 137, 2168-2179, (2015).
- 11 Hunaidi O., Chu W.T., Acoustical characteristics of leak signals in water distribution pipes, *Applied Acoustics*, 58, 235 - 254, (1999).
- 12 Gao Y., Brennan, M. J., Liu Y., et al, Improving the shape of the cross-correlation function for leak detection in a plastic water distribution pipe using acoustic signals, *Applied Acoustics* (under review)
- 13 Pinnington, R. J., Briscoe, A. R., Externally applied sensor for axisymmetric waves in a fluid filled pipe, *Journal of Sound and vibration*, 173, 503-516, (1994).